

# A robust sagittal plane hexapedal running model with serial elastic actuation and simple periodic feedforward control

Martin Görner and Alin Albu-Schäffer

**Abstract**—In this article we present a sagittal plane, sprawled posture hexapedal running model with distributed body inertia, massless legs and serial elastic actuation at the hips as well as along the telescoping legs. We show by simulation that simple, periodic, feedforward controlled actuation is sufficient to obtain steady period 1 running gaits at twice the actuation frequency. We observe a nearly linear relation of average running speed and actuation frequency. The ground reaction profiles of the legs show leg specialization as observed in running insects. Interleg phasing has a strong influence on the foot fall sequence and thus the overall body dynamics. While the single leg ground reaction force profiles show little dependency on interleg actuation phase the total reaction force does. Thus, depending on the interleg actuation phase body motions without flight phase are observed as well as body motions and total ground reaction forces that show similarities to those obtained for the spring loaded inverted pendulum model. Further, we show that including leg damping and a ground friction model the periodic orbits have a large region of attraction with respect to the initial conditions. Additionally, the model quickly rejects step up and step down disturbances as well as force impulses. Finally, we briefly discuss the energetics of the hexapedal running model.

## I. INTRODUCTION

In nature, hexapedal runners such as cockroaches show impressive dynamical stability and robustness with respect to disturbances. According to experimental studies they are able to traverse highly unstructured terrain at very high velocities. Hereby, they cross obstacles and dents larger than their hip height with little changes of running speed and neural activation pattern [5]. Therefore, biologists hypothesize that the remarkable robustness and stability of rapidly running cockroaches results from self-stabilizing properties of their mechanical structure in combination with an appropriate periodic feedforward controlled actuation [7]. Inspired by their natural counterparts, hexapedal robotic platforms like RHex [12] or the Sprawl robots from Stanford [3] have been built that exploit such self-stabilizing mechanisms using passively compliant, underactuated legs and feedforward control. With regard to experimental data on ground reaction forces and kinematics of running cockroaches as well as the above mentioned robots, different conceptual mathematical models have been developed to test hypotheses on the underlying structure of robust dynamic locomotion.

The work presented in this article is also motivated by the question of how to embed self-stabilizing fast locomotion capabilities in hexapedal robots. Our underlying assumption is the existence of compliant mechanical configurations that

together with proper periodic feedforward excitation result in running motions characterized as phase synchronized, coupled, nonlinear oscillations. We approach the identification of possible mechanical structures by modeling the sagittal plane dynamics of running hexapods. Hereby we use a body with distributed mass, six massless, actuated, compliant legs and explicitly include body pitch motions. For our model we assume that it is possible to capture the basic leg functionality by combining a feedforward controlled telescoping serial elastic actuator along the leg with a feedforward controlled rotating serial elastic actuator at the hip. Following these assumptions we identify asymmetric kinematic configurations, suitable parameter sets and simple periodic excitation that result in stable sagittal plane locomotion. We perform extensive simulation studies to show the occurrence of periodic orbits and to quantify their region of attraction. Further, we show that the running velocity is proportional to the excitation frequency and that the ground reaction forces of our model indicate leg specialization as it is observed in insects [6]. Introducing a phase shift in between front, middle and hind leg actuation of the same tripod we observe variations of the center of mass dynamics. These range from dynamics without a flight phase but with a short double support by both tripods towards dynamics that are qualitatively similar to the spring loaded inverted pendulum model. Considering the power flow of the system we show that the springs act as storage elements that mainly bridge the phase shift of motor power and leg power rather than increasing efficiency.

The article proceeds as follows. In Sect. II we briefly discuss related literature and introduce our system model as well as a dimensionless version. In Sect. III we present simulation studies and analyze the model behavior with respect to the occurrence of periodic orbits, their region of attraction and the robustness against disturbances. Further, we briefly comment on the energetics of our model. Finally in Sect. IV, we conclude our work.

## II. SAGITTAL PLANE HEXAPEDAL MODEL

A variety of models with different levels of complexity has been developed to capture the hybrid dynamics of animal locomotion. The most prominent example is the spring loaded inverted pendulum (SLIP), a simple conservative spring mass model for sagittal plane dynamics. The SLIP model predicts the basic motions and whole body ground reaction forces for a wide variety of animals [2] including hexapedal runners [8] and is considered as a template for animal locomotion. The lateral leg spring (LLS) model [13], [14] transfers the SLIP properties into the horizontal plane

M.Görner and A.Albu-Schäffer are with the Robotics and Mechatronics Center at the German Aerospace Center (DLR), Oberpfaffenhofen, Germany, martin.goerner@dlr.de

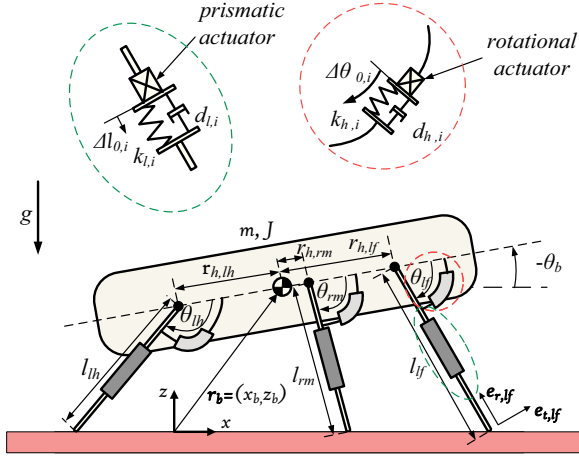


Fig. 1. Hexapod model with left tripod in support

but additionally includes yaw motions as a third degree of freedom (DOF). Both models, the SLIP and the LLS, show self-stable periodic orbits and capture the basic behavior of hexapedal locomotion. In addition to those simple models more complex planar hexapedal running models exist that include a body with mass moment of inertia, six massless, compliant legs and different modes of actuation. One example for the horizontal plane is the model presented by Seipel [15] et al. that achieves stable and robust locomotion using six telescoping compliant legs of which the force-free length and the location of the hip attachment points along the body are prescribed functions of time. These functions have been calculated such that ideal body motions match desired ground reaction force profiles. For the sagittal plane Saranlı [11] and Ankaralı et al. [1] present models with passive, compliant legs and rigid hip actuation that either employ tuned feedforward hip joint trajectories or try to embed SLIP like behavior by control. Clark et al. [4] use a multi-body approach to model the dynamics of their Sprawl type robots with pneumatically actuated, telescoping legs and passive, compliant hips. By extensive simulation they show that a sprawled posture improves robustness and stability of periodic running gaits. Close to our approach but applied to single leg hopping, Remy [10] employs a planar model with distributed masses and serial elastic actuation with a focus on comparing the effect of cost functions on locomotion efficiency in an optimal control framework.

#### A. System model

Our model for sagittal plane hexapedal running consists of a body with mass  $m$  and mass moment of inertia  $J$ , six massless, serial elastic actuated, telescoping legs and serial elastic actuated, rotating hips. A viscous damper is included in parallel to each spring. The legs are arranged in a sprawled posture. Front, middle and hind legs each have a different length. All hip joints are collinear with the body center of mass which is placed slightly behind the hip joint of the middle leg. A second order slip model is implemented for each foot that can be activated or deactivated. Upon

activation the slip model moves the foot contact point once the ground reaction force leaves the friction cone. If it is deactivated the foot position is fixed during stance until the lift off condition is fulfilled. Two tripods consisting of left front, left hind and right middle leg (left tripod) as well as right front, right hind and left middle leg (right tripod) are controlled  $180^\circ$  out of phase with a single frequency periodic feedforward pattern. Hereby, the actuation changes the force free length of the leg and hip springs following a sine based pattern for the telescoping legs and a cosine based pattern for the rotating hip joints. The equations of motion of our hexapedal model are the following,

$$m\ddot{\mathbf{r}}_b = \mathbf{f}_g + \sum_{i=0}^6 \mathbf{f}_{l,i}, \quad (1)$$

$$J\ddot{\theta}_b = \sum_{i=0}^6 -\tau_{h,i} + \sum_{i=0}^6 (-r_{h,i}\sin(\theta_b)f_{lx,i} - r_{h,i}\cos(\theta_b)f_{lz,i}) \quad (2)$$

$$\tau_{h,i} = \begin{cases} -(k_{h,i}\Delta\theta_i + d_{h,i}\dot{\Delta}\theta_i) & : c_i = 1 \\ 0 & : c_i = 0 \end{cases}, \quad (3)$$

$$\mathbf{f}_{l,i} = \begin{cases} -(k_{l,i}\Delta l_i + d_{l,i}\dot{\Delta}l_i)\mathbf{e}_{r,i} + \frac{\tau_{h,i}}{l_i}\mathbf{e}_{t,i} & : c_i = 1 \\ \mathbf{0}_{2 \times 1} & : c_i = 0 \end{cases} \quad (4)$$

Herein,  $\mathbf{r}_b = (x_b, z_b)$  is the planar position of the body center of mass (COM) with respect to the world coordinate system. The vector  $\mathbf{f}_g$  represents the gravity force acting on the COM and  $\mathbf{f}_{l,i}$ ,  $i = 1 \dots 6$  are the ground reaction forces of the legs.  $\theta_b$  is the pitch angle of the body and  $\tau_{h,i}$  are the torques at the hip joints of the respective legs. The distance between the hip joint of the  $i$ th leg and the COM is given by  $r_{h,i}$  which is positive for the hip being located in front of the COM and negative for the hip being located behind the COM. The parameters  $k_{h,i}$  and  $d_{h,i}$  are the spring and damping constant of the  $i$ th hip joint while  $k_{l,i}$  and  $d_{l,i}$  are the spring and damping constant of the  $i$ th leg.  $\mathbf{e}_{r,i}$  is the radial unit vector of leg  $i$  that is directed along the leg towards the hip.  $\mathbf{e}_{t,i}$  is the tangential unit vector of the respective leg that results from rotating  $\mathbf{e}_{r,i}$   $90^\circ$  clockwise. The discrete state  $c_i = 1$  indicates ground contact of leg  $i$ . The touch down (TD) and lift off (LO) conditions of a leg are TD:  $z_b - r_{h,i}\sin(\theta_b) - l_{0,i}(t)\sin(\theta_{0,i}(t) + \theta_b) \leq 0$  and LO:  $f_{lz,i} = 0$ ,  $\dot{f}_{lz,i} < 0$ . The deflection of hip and leg spring is given by  $\Delta\theta_i$  and  $\Delta l_i$ , respectively, which are calculated according to

$$\Delta\theta_i = \theta_i - \theta_{0,i} - \frac{\Delta\theta_{0,i}}{2}(1 - \cos(\phi(t) + \Delta\phi_i)), \quad (5)$$

$$\Delta l_i = l_i - l_{0,i} - \Delta l_{0,i}\sin(\phi(t) + \Delta\phi_i). \quad (6)$$

The terms  $\theta_{0,i}(t) = \theta_{0,i} + \frac{\Delta\theta_{0,i}}{2}(1 - \cos(\phi(t) + \Delta\phi_i))$  and  $l_{0,i}(t) = l_{0,i} + \Delta l_{0,i}\sin(\phi(t) + \Delta\phi_i)$  are the force free length of hip and leg spring consisting of a fixed and a time varying component. The fixed components of the rotational hip springs,  $\theta_{0,i}$  are determined manually. In contrast, the fixed components of the translational leg springs,  $l_{0,i}$  are calculated such that the feet touch ground for a configuration with a COM height  $h_0$ , zero body pitch and leg angles

according to  $\theta_i = \theta_{0,i}$ . The time varying part of the force free length of the springs is the feedforward control signal with a time and frequency dependent phase,  $\dot{\phi}(t) = \omega$ , and a leg specific fixed phase shift,  $\Delta\phi_i$ . This leg specific phase shift is composed of interleg phase shifts within the same tripod group ( $\phi_{lf} = \phi_{lh} + 2 \cdot \phi_0$  and  $\phi_{rm} = \phi_{lh} + \phi_0$ , where  $\phi_0$  is a constant) and a  $180^\circ$  phase shift with respect to the opposite tripod group. The subscripts *lf*, *rm* and *lh* indicate the specific legs of the left tripod, i.e. left front, right middle and left hind respectively. The right tripod follows the same naming conventions.

To be more realistic with respect to slippage we include a second order slip model for the feet which can be activated or deactivated during simulation. If the slip model is activated a small mass is assigned to each foot in stance. Once the horizontal ground reaction force is larger than the static friction force the difference of both forces accelerates the foot mass and thus shifts the ground contact point of the foot. If the horizontal ground reaction force returns into the friction cone the foot motion is decelerated.

### B. Dimensionless system model

To obtain more general results we introduce a dimensionless version of the model presented in the previous section. For this purpose we normalize the equations following the procedure presented by Hof [9]. The characteristic parameters for scaling are the body mass,  $m$ , and the height of the center of mass,  $h_0$ , as described above. Thus, with the tilde symbolizing dimensionless quantities, the equations of motion (1) and (2) take the following form.

$$\ddot{\mathbf{r}}_b = \begin{pmatrix} 0 \\ 1 \end{pmatrix} + \sum_{i=0}^6 \tilde{\mathbf{f}}_{l,i}, \quad (7)$$

$$\tilde{J}\ddot{\theta}_b = \sum_{i=0}^6 -\tilde{\tau}_{h,i} + \sum_{i=0}^6 (-\tilde{r}_{h,i} \sin(\tilde{\theta}_b) \tilde{f}_{lx,i} - \tilde{r}_{h,i} \cos(\tilde{\theta}_b) \tilde{f}_{lz,i}) \quad (8)$$

We note that all derivatives indicated by dots are now taken with respect to the dimensionless time,  $\tilde{t}$ . In order to obtain dimensionless equivalents of equations (3) to (6) their structure is kept, but all states, parameters and time are replaced by their dimensionless version. Table I gives the relations of all quantities and their dimensionless counterparts.

## III. SIMULATION STUDIES

In this section we demonstrate and analyze the behavior of our hexapedal running model by use of simulations. For this purpose we use a Matlab/Simulink implementation of the model and the variable step solver ODE45. First, we demonstrate the appearance of periodic orbits and show the relation of feedforward actuation frequency and running speed. Next, we demonstrate how a phase shift within the actuation of the legs of one tripod changes the overall dynamic behavior and the footfall sequence. Following, we present estimates for the region of attraction for SLIP like running with respect to the initial conditions. Finally, we show that the model is

TABLE I  
PHYSICAL QUANTITIES AND THEIR DIMENSIONLESS COUNTERPARTS

Quantity	Dimensionless Quantity	Definition
time, $t$	$\tilde{t}$	$:= t/\sqrt{h_0/g}$
length, $l$	$\tilde{l}$	$:= l/h_0$
position, $\mathbf{r}$	$\tilde{\mathbf{r}}$	$:= \mathbf{r}/h_0$
velocity, $\dot{\mathbf{r}}$	$\dot{\tilde{\mathbf{r}}}$	$:= \dot{\mathbf{r}}/\sqrt{gh_0}$
acceleration, $\ddot{\mathbf{r}}$	$\ddot{\tilde{\mathbf{r}}}$	$:= \ddot{\mathbf{r}}/g$
angle, $\theta$	$\tilde{\theta}$	$:= \theta$
angular velocity, $\dot{\theta}$	$\dot{\tilde{\theta}}$	$:= \dot{\theta}\sqrt{h_0/g}$
angular acceleration, $\ddot{\theta}$	$\ddot{\tilde{\theta}}$	$:= \ddot{\theta}h_0/g$
mass moment of inertia, $J$	$\tilde{J}$	$:= J/(mh_0^2)$
translational spring, $k_l$	$\tilde{k}_l$	$:= k_l h_0/mg$
rotational spring, $k_h$	$\tilde{k}_h$	$:= k_h/mgh_0$
translational damping, $d_l$	$\tilde{d}_l$	$:= d_l\sqrt{h_0/g}/m$
rotational damping, $d_h$	$\tilde{d}_h$	$:= d_h/(m\sqrt{gh_0^3})$
force, $\mathbf{f}$	$\tilde{\mathbf{f}}$	$:= \mathbf{f}/(mg)$
torque, $\tau$	$\tilde{\tau}$	$:= \tau/(mgh_0)$

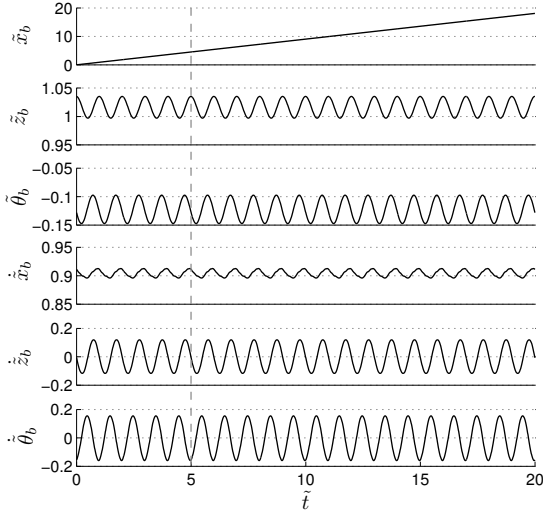
TABLE II  
DIMENSIONLESS MODEL PARAMETERS

Body	$\tilde{J}$	0.6944		
Legs:	front	middle	hind	
$\tilde{r}_h$	0.8333	0.1667	-0.8333	
$\tilde{l}_0$	1.1547	1.0154	1.0154	
$\Delta\tilde{l}_0$	0.25	0.25	0.25	
$\tilde{\theta}_0$	1.0472 (60°)	1.3963 (80°)	1.7453 (100°)	
$\Delta\tilde{\theta}_0$	0.6109 (35°)	0.6109 (35°)	0.7854 (45°)	
$\tilde{k}_l$	2.9358	2.9358	2.9358	
$\tilde{d}_l$	0	0	0	
$\tilde{k}_h$	0.6796	0.6796	0.6796	
$\tilde{d}_h$	0	0	0	
$\tilde{\phi}_0$	0	0	0	

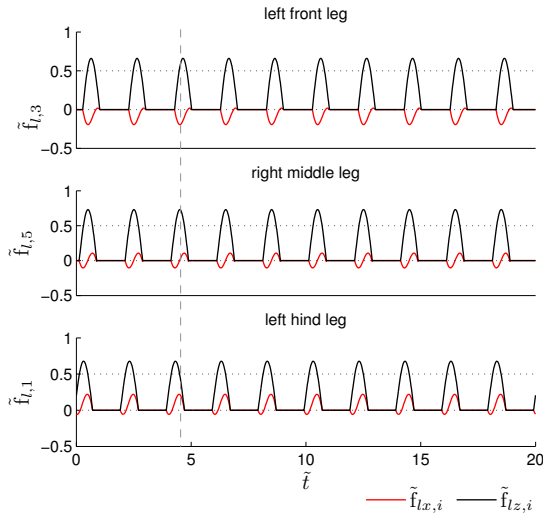
robust with respect to step disturbances and briefly discuss the energetics. Throughout the section all results are given in their more general dimensionless form.

### A. Periodic orbits

For a certain range of actuation frequencies  $\tilde{\omega}/2\pi$  and model parameters the hexapedal running model converges to stable periodic orbits. These orbits are period 1 with respect to the body. Due to the alternating actuation of left and right tripod, all body states (except the horizontal displacement) oscillate at twice the actuation frequency. We find fixed points of the return map at ‘‘apex’’ (maximum vertical displacement and zero vertical velocity) by simulation once the body states remain within an error region of  $10^{-5}$  for 100 successive half strides. Hereby, a half stride covers the stance phase of left or right tripod. The dimensionless model parameters used throughout the simulations are given in table



(a)



(b)

Fig. 2. Steady running gait: (a) trajectories; (b) ground reaction forces, ( $\tilde{\omega}/2\pi = 0.5$ ,  $\tilde{\phi}_0 = 0$ ,  $\tilde{d}_l = 0$ ,  $\tilde{d}_h = 0$ )

II. Left and right tripod are actuated  $180^\circ$  out of phase while the legs within the same tripod are perfectly actuated in phase ( $\tilde{\phi}_0 = 0$ ). Leg and hip damping constants are all set to zero. As can be seen in Figure 2(a), the body states converge to a steady period 1 running gait. Horizontal kinetic energy and gravitational potential energy are in phase as is indicated by the dashed vertical line that runs through the maximum of horizontal velocity and vertical displacement. Figure 2(b) shows the ground reaction forces of the legs of the left tripod, which are equivalent for the right tripod. The feet show sequential touchdown starting with the hind leg followed by the middle and the front leg. The stance duration and vertical force component are almost equal for all legs while specialization is observed for the horizontal force component. Similar to observations on cockroaches

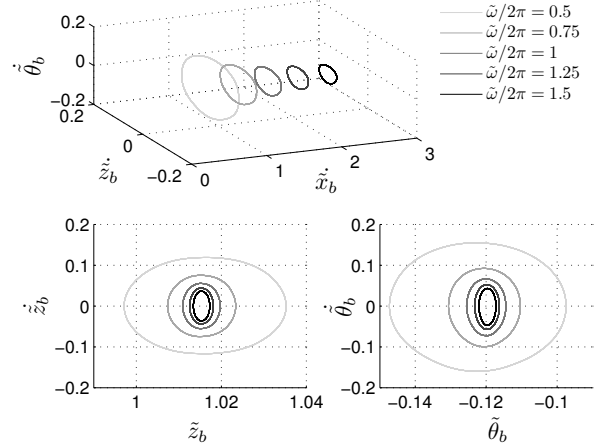


Fig. 3. Periodic orbits for running at different feedforward actuation frequencies, ( $\tilde{\phi}_0 = 0$ ,  $\tilde{d}_l = 0$ ,  $\tilde{d}_h = 0$ )

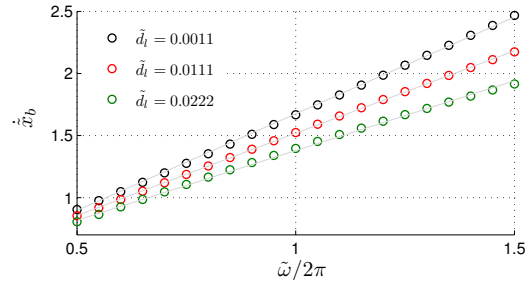


Fig. 4. Average forward velocity with respect to the feedforward actuation frequency for different values of leg damping, ( $\tilde{\phi}_0 = 0$ ,  $\tilde{d}_h = 0$ )

[6], the front leg mainly decelerates the body, the middle leg first decelerates and then accelerates the body and the hind leg dominantly accelerates the body. In Fig. 3 we show the periodic orbits in state space and their dependency on actuation frequency. Increasing the feedforward actuation frequency leads to larger forward velocity and decreasing amplitudes of all other periodic states. As can be seen in Fig. 4 the average forward velocity increases almost linearly with actuation frequency for zero leg and hip damping. Increasing the leg damping leads to smaller average forward velocities and slightly increased bending of the velocity-frequency curve but has only little qualitative influence on the shape of the body trajectories and ground reaction forces patterns. For steady running gaits the second order slip model applied to the foot ground interaction was never active since horizontal forces always were within the friction cone.

### B. Interleg phasing

An interesting property of the model can be observed by introducing a larger phase shift of  $\tilde{\phi}_0$  in between middle and hind leg as well as  $2 \cdot \tilde{\phi}_0$  in between front and hind leg of the same tripod. Keeping the contra-lateral legs  $180^\circ$  out of phase this new phase shift influences the foot fall sequence and the observed dynamic behavior. Figure 5 displays the leg specific and the total ground reaction forces for three

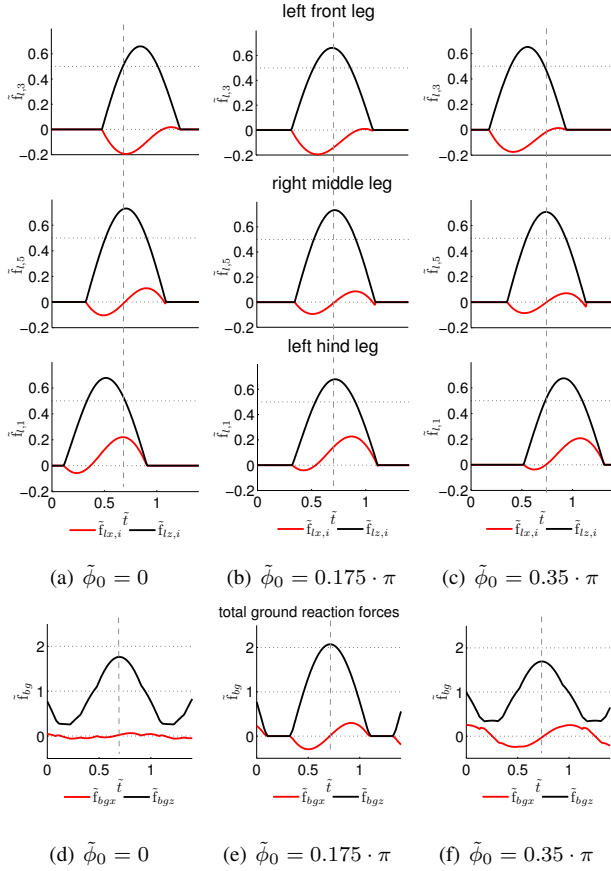


Fig. 5. Single leg ground reaction forces,(a)-(c), and total ground reaction forces,(d)-(f) , for different interleg phase shift values, ( $\tilde{\omega}/2\pi = 0.5$ ,  $\tilde{d}_l = 0$ ,  $\tilde{d}_h = 0$ )

different phase shift values. Increasing the phase shift from zero at constant actuation frequency, the foot fall sequence changes from leading hind leg via simultaneous touch down towards leading front leg. Apparently, this has negligible influence on stance duration and force characteristics of the single leg but shifts their relative phase. Nevertheless, this relative phase shift of single leg ground reaction forces changes the overall dynamic behavior as can be observed in Fig. 5(d)-(f) as well as Fig. 6. While experiencing no flight phase, small horizontal forces and thus small variations of forward velocity for zero phase shift, the model shows qualitatively SLIP like behavior for a phase shift that results in simultaneous touch down. Hereby, the simulations reveal a flight phase and very smooth ground reaction force profiles similar to those observed for the spring loaded inverted pendulum. Additionally, the body shows only very small pitch oscillations. Increasing the phase shift further, the flight phase disappears but the model shows larger horizontal force variations than for zero phase shift.

### C. Transient dynamics, region of attraction and disturbance rejection

Since initial conditions are usually not part of the periodic orbit or the model is subject to external disturbances, transient dynamics play an important role. For those dynamics

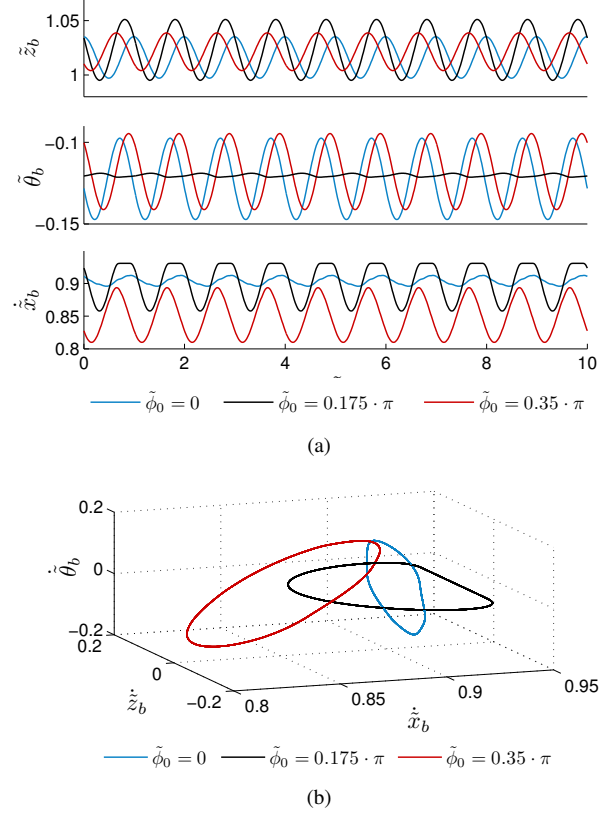


Fig. 6. Trajectories and periodic orbits for different interleg phase shifts, ( $\tilde{\omega}/2\pi = 0.5$ ,  $\tilde{d}_l = 0$ ,  $\tilde{d}_h = 0$ )

leg damping and the second order slip model applied to the foot ground interaction are included. During these transition processes the model with zero slip and zero leg damping stabilizes quickly for a wide range of initial conditions but displays horizontal force peaks at the end of a step that violate friction constraints. This behavior can be removed by allowing the feet to slip according to the model presented above. In combination with small leg damping the model quickly transitions to its periodic orbit without violating friction constraints as displayed in Fig. 7. Following, we present regions of attraction for the hexapedal model parametrized such that it displays SLIP like behavior ( $\tilde{\phi}_0 = 0.175 \cdot \pi$ ). Starting at apex with various initial velocities, Fig. 8 shows the number of full strides taken until the model settles to its steady periodic gait. Each of the diagrams displays a total of 400 simulations along an equidistant grid of initial vertical and horizontal velocity. To demonstrate the influence of leg damping two different values have been assigned,  $\tilde{d}_l = 0.0011$  for the complete left column and  $\tilde{d}_l = 0.0111$  for the complete right column. For Fig. 8(a) and (b) all other initial states correspond to the apex states of the steady periodic orbit. In subsequent figures additional initial conditions have been changed. In Fig. 8(c) and (d) the initial height is raised by 0.2, in Fig. 8(e) and (f) the initial angle of the body is zero and in Fig. 8(g) and (h) the initial angular velocity of the body is set to 0.5. The plots show that the fixed point

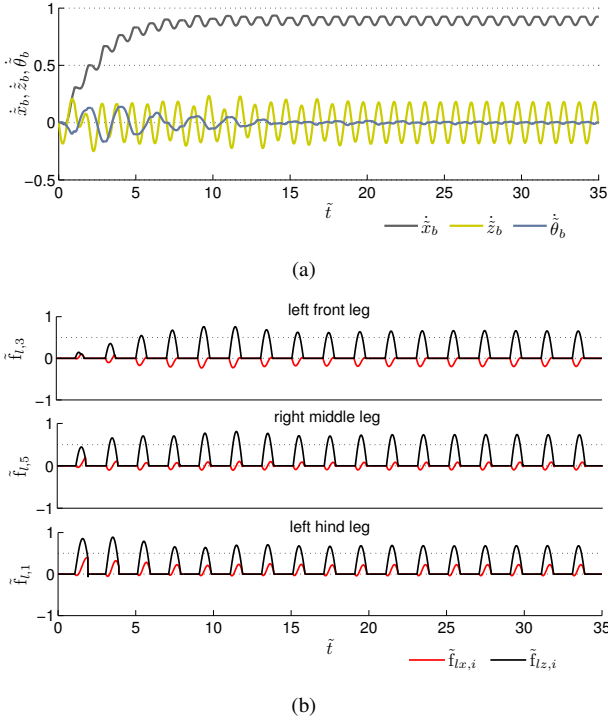


Fig. 7. Trajectories for starting at apex (fixed point states) with zero initial horizontal and vertical velocity, ( $\tilde{\omega}/2\pi = 0.5$ ,  $\tilde{\phi}_0 = 0.175 \cdot \pi$ ,  $\tilde{d}_l = 0.0111$ ,  $\tilde{d}_h = 0$ )

is attractive for a wide variety of initial forward velocities. Further, we see that higher initial downward velocity does not result in stable motion for larger initial angular offsets. Clearly, leg damping enlarges the region of attraction for all initial conditions and reduces the number of transition strides. Figure 9 and the video attachment give an example for the ability of the model to reject step disturbances.

#### D. Energetics

Finally, we want to comment on the energetic behavior of the model. As shown in Fig. 10 the actuators have to provide or absorb substantial power in order to inject or to remove energy from the system. Hereby, the motors mirror the functional behavior of the legs. The prismatic actuator of each front leg dominantly absorbs energy, while the prismatic actuator of each hind leg mainly injects energy and the prismatic actuator of each middle leg does both. As can be seen, the springs obviously function as storage elements that mainly bridge the evident phase shift between actuator and leg power. The hips show a behavior opposite to the legs. The front hip joints provide energy while the hind hip joints absorb it. The data suggest that providing efficiency is not the core functionality of the springs. For example, running at an actuation frequency of  $\tilde{\omega}/2\pi = 0.5$ , with interleg phase shifts of  $\tilde{\phi}_0 = 0.175 \cdot \pi$  and zero leg damping results in a steady periodic motion that for a half stride shows 8.17% fluctuation of the total mechanical energy of the body with respect to its maximum value. Across the same time span all motors inject and consequently also remove 15.92 % of the

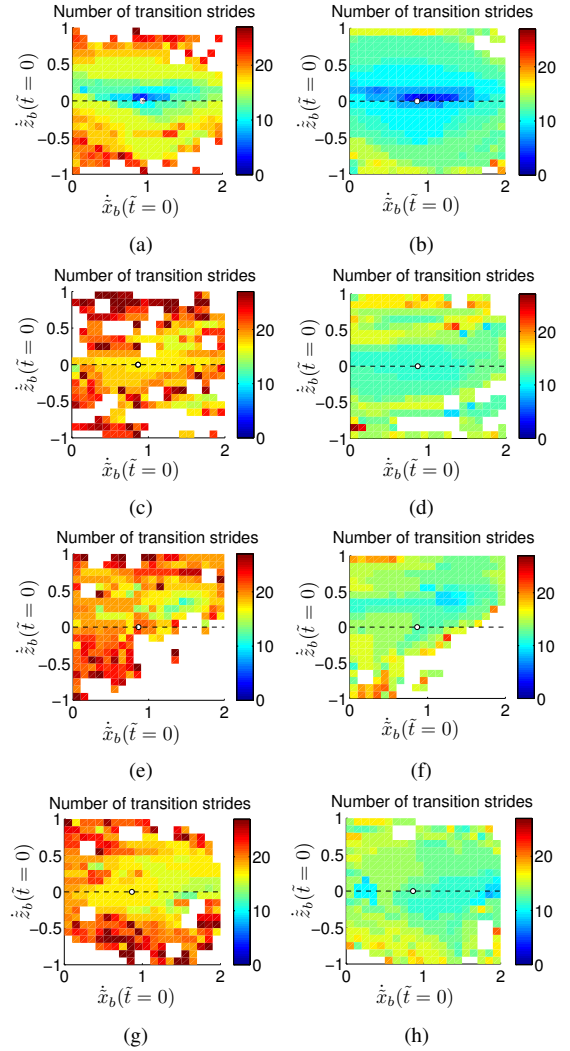


Fig. 8. Number of full strides until the transient dynamics settles to the steady periodic orbit with respect to initial velocities: leg damping is  $\tilde{d}_l = 0.0011$  for the left column and  $\tilde{d}_l = 0.0111$  for the right column; the fixed point at apex indicated by a white dot is,  $(\dot{x}_b, \dot{z}_b, \dot{\theta}_b, \tilde{z}_b, \tilde{\theta}_b, \tilde{\phi})^* = (0.9309, 0, 0.0023, 1.0511, -0.1211, 2.5477)$  for the left column and  $(\dot{x}_b, \dot{z}_b, \dot{\theta}_b, \tilde{z}_b, \tilde{\theta}_b, \tilde{\phi})^* = (0.8657, 0, 0.0058, 1.0554, -0.121, 2.4534)$  for the right column; apart from the varied initial velocities the other initial states correspond to: (a), (b) - the fixed point at apex; (c), (d) - the fixed point at apex but with increased initial height ( $\tilde{z}_b(\tilde{t} = 0) = \tilde{z}_b^* + 0.2$ ); (e), (f) - the fixed point at apex but with zero initial angle; (g), (h) - the fixed point at apex but with increased initial angular velocity ( $\tilde{\theta}_b(\tilde{t} = 0) = 0.5$ )

maximum mechanical energy of the body. Thus, the motors provide more power than necessary to only account for the net power exchange of the body. In Fig. 11 we show the cost of transport (COT) for one full stride as a function of actuation frequency and leg damping. Hereby, the COT is the sum of positive work performed by all actuators during one stride divided by weight and distance traveled. This is computed from dimensionless quantities by,

$$\text{COT} = \frac{\int_0^{\tilde{T}} \sum_{i=1}^6 (\max(\tilde{f}_{tr,i} \dot{l}_{0,i}, 0) + \max(\tilde{\tau}_{h,i} \dot{\theta}_{0,i}, 0)) d\tilde{t}}{\Delta \tilde{x}_{b, stride}} \quad (9)$$

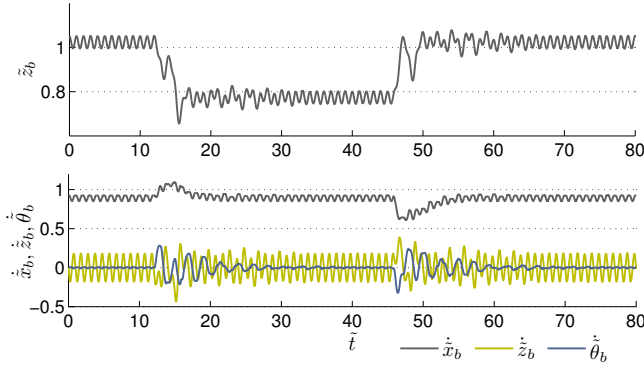


Fig. 9. Trajectories for  $\Delta\tilde{h} = 0.25$  (25%) step down and step up disturbances, ( $\tilde{\omega}/2\pi = 0.5$ ,  $\tilde{\phi}_0 = 0.175 \cdot \pi$ ,  $\tilde{d}_l = 0.0111$ ,  $\tilde{d}_h = 0$ )

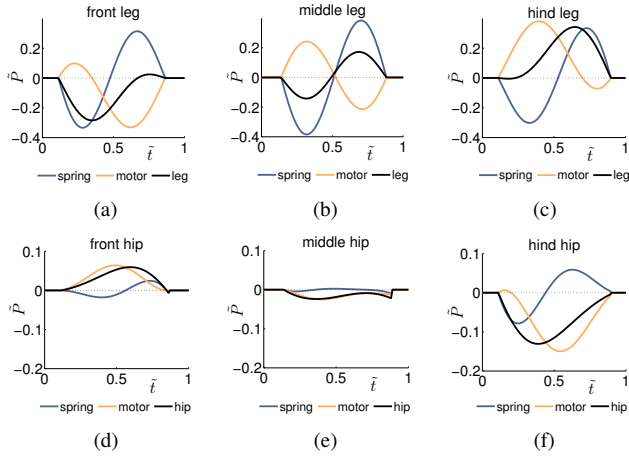


Fig. 10. Power over one stride for the telescoping legs, (a)-(c), and the rotating hips, (d)-(f), ( $\tilde{\omega}/2\pi = 0.5$ ,  $\tilde{\phi}_0 = 0.175 \cdot \pi$ ,  $\tilde{d}_l = 0$ ,  $\tilde{d}_h = 0$ )

Herein,  $\tilde{f}_{lr,i}$  is the radial force component along the leg computed from leg spring and damper. The substantial amount of negative work performed by the actuators is not considered in the COT since this energy could be regenerated or just lost as heat. From the diagram in Fig. 11 we observe that for zero leg damping the COT shows little dependency on the actuation frequency and thus running speed. Further, the COT grows almost linearly with leg damping for a fixed actuation frequency, while the slope of this relation increases for higher frequencies. Additionally, interleg phasing appears to have minor influence on the COT as well as leg slippage which does not appear at steady state running.

#### IV. CONCLUSIONS AND FUTURE WORK

In this article we have studied the behavior of a sagittal plane hexapedal running model with serial elastic actuation and simple periodic feedforward control. We have shown that kinematic configurations and parameter sets exist that result in stable period 1 running motions at twice the actuation frequency. Average running speed is almost linearly related to the actuation frequency. Leg damping strongly increases the robustness with respect to the initial conditions, step disturbances and force impulses. Changing interleg phasing

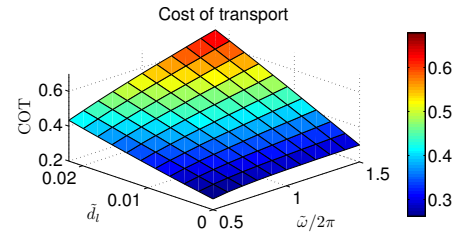


Fig. 11. Cost of transport with respect to leg damping and actuation frequency ( $\tilde{\phi}_0 = 0.175 \cdot \pi$ ,  $\tilde{d}_h = 0$ )

allows influencing the foot fall sequence and produces different overall dynamic behaviors with or without flight phases. In this configuration the springs mainly modulate the power flow and do not increase efficiency. The motors produce substantially more work than the pure body dynamics would require. The cost of transport grows approximately linearly with leg damping for a fixed actuation frequency and shows little dependency on the interleg phasing. Currently, we investigate the extension of the model to 3D, perform a detailed sensitivity analysis with respect to parameters and evaluate the limitations of the model in greater detail. In future we want to build an experimental robotic platform to verify the results obtained for our model and want to evaluate how to transfer the functional behavior to articulated legs.

#### V. ACKNOWLEDGMENTS

We thankfully acknowledge the support of this work by the Helmholtz Alliance ROBEX.

#### REFERENCES

- [1] M. Ankarali and U. Saranli, "Control of underactuated planar pronking through an embedded spring-mass hopper template," *Auton. Robot.*, 2011.
- [2] R. Blickhan and R. Full, "Similarity in multilegged locomotion: Bouncing like a monopode," *J. Comp. Physiol. A*, 1993.
- [3] J. Cham, S. Bailey, J. Clark, R. Full, and M. Cutkosky, "Fast and robust: Hexapedal robots via shape deposition manufacturing," *Int. J. Robotics Res.*, 2002.
- [4] J. Clark and M. Cutkosky, "The effect of leg specialization in a biomimetic hexapedal running robot," *J. Dyn. Sys., Meas., Control*, 2005.
- [5] R. Full, K. Autumn, J. Chung, and A. Ahn, "Rapid negotiation of rough terrain by the death-head cockroach," *Am. Zool.*, 1998.
- [6] R. Full, R. Blickhan, and L. Ting, "Leg design in hexapedal runners," *J. Exp. Biol.*, 1991.
- [7] R. Full and D. Koditschek, "Templates and anchors: neuromechanical hypotheses of legged locomotion on land," *J. Exp. Biol.*, 1999.
- [8] R. Full and M. Tu, "The mechanics of six-legged runners," *J. Exp. Biol.*, 1990.
- [9] L. Hof, "Scaling gait data to body size," *Gait and Posture*, 1996.
- [10] C. Remy, K. Buffinton, and R. Siegwart, "Comparison of cost functions for electrically driven running robots," in *IEEE Int. Conf. on Robotics and Automation*, St Paul, MN, USA, 2012.
- [11] U. Saranli, "Dynamic locomotion with a hexapod robot," Ph.D. dissertation, The University of Michigan, 2002.
- [12] U. Saranli, M. Buehler, and D. Koditschek, "Rhex: A simple and highly mobile hexapod robot," *Int. J. Robotics Res.*, 2001.
- [13] J. Schmitt and P. Holmes, "Mechanical models for insect locomotion: dynamics and stability in the horizontal plane i. theory," *Biol. Cybern.*, 2000.
- [14] —, "Mechanical models for insect locomotion: dynamics and stability in the horizontal plane ii. application," *Biol. Cybern.*, 2000.
- [15] J. Seipel, P. Holmes, and R. Full, "Dynamics and stability of insect locomotion: A hexapedal model for horizontal plane motions," *Biol. Cybern.*, 2004.